Supplementary materials for

Bacteria-responsive cytoderm drug delivery system

Chenmeng Zhou[1], Yue Zhang[1], Bo Tian[2], Yue Yu[1], Dongxiao Li[2], Bingbing Wu[1], Wenju Chang[2], Tongguo Shi[3], Fang Xu[1]*, Jinyu Bai[2]*, Chao Wang[1]*

[1] Institute of Functional Nano & Soft Materials (FUNSOM), Jiangsu Key Laboratory for Carbon-based Functional Materials and Devices, Soochow University, Suzhou, Jiangsu 215123, China

[2] Department of Orthopedics, The Second Affiliated Hospital of Soochow University, Suzhou, Jiangsu 215123, China

[3] Jiangsu Institute of Clinical Immunology, The First Affiliated Hospital of Soochow University Suzhou 215000, China

* Corresponding author: Jinyu Bai: baijy@suda.edu.cn, Chao Wang: cwang@suda.edu.cn, Fang Xu: fangx@suda.edu.cn

Content:

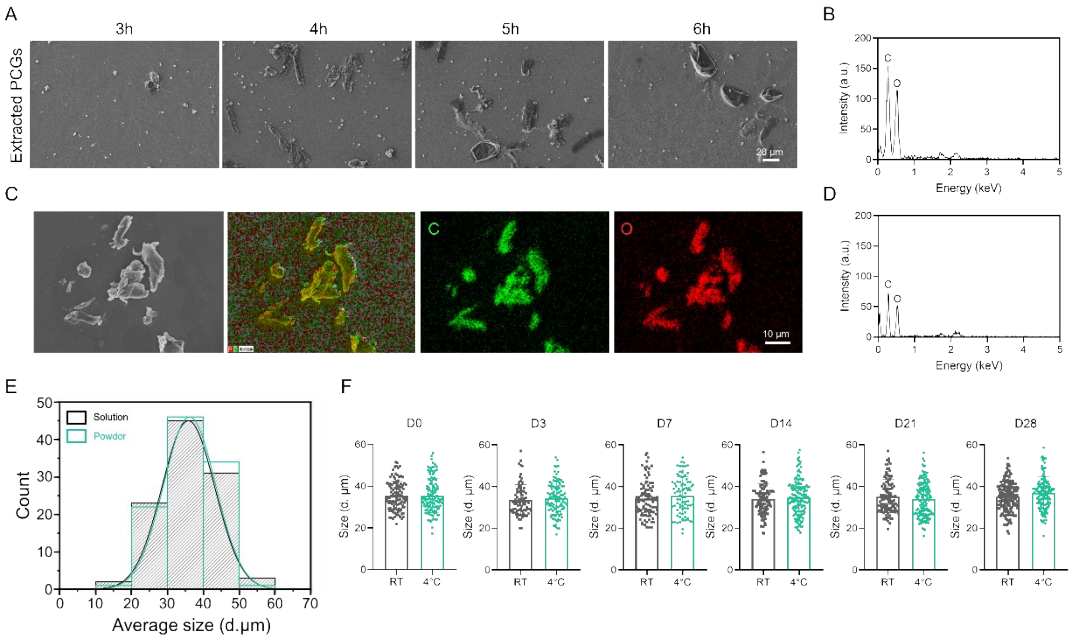

Figure S1. Preparation and characterization of PCGs. A. Representative SEM images of PCGs obtained by extraction with different processing time. Scale bar=20 μm. **B.** The corresponding energy dispersive X-ray energy spectrum of PCGs. **C.** The corresponding element distribution of cellulose powder. Scale bar=10 μm. **D.** The corresponding energy dispersive X-ray energy spectrum of purchased cellulose. **E.** The size distribution of PCGs powder and solution (n>100). **F.** Size distribution of PCGs in PBS at room temperature and 4 °C for different time. The data are presented as means ± SD.

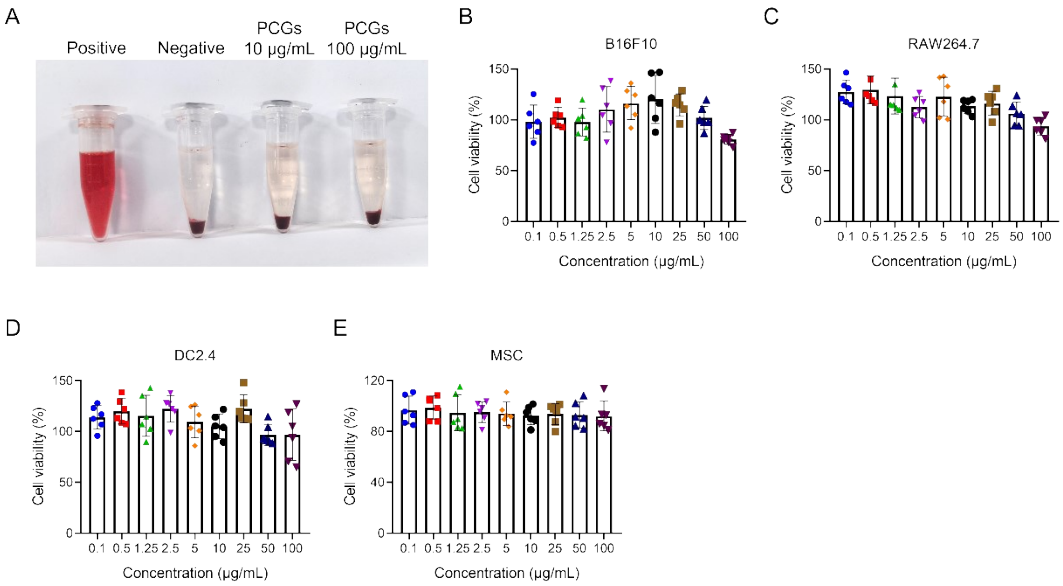

Figure S2. Biocompatibility of PCGs. A. Representative picture of hemolysis test for PCGs. **B-E.** Cytotoxicity of PCGs. Cell viability of B16F10 cells **(B)**, RAW264.7 **(C)**, DC2.4 **(D)** and mesenchymal stem cell (MSC) **(E)** treated with PCGs (n=6). The data are presented as means ± SD.

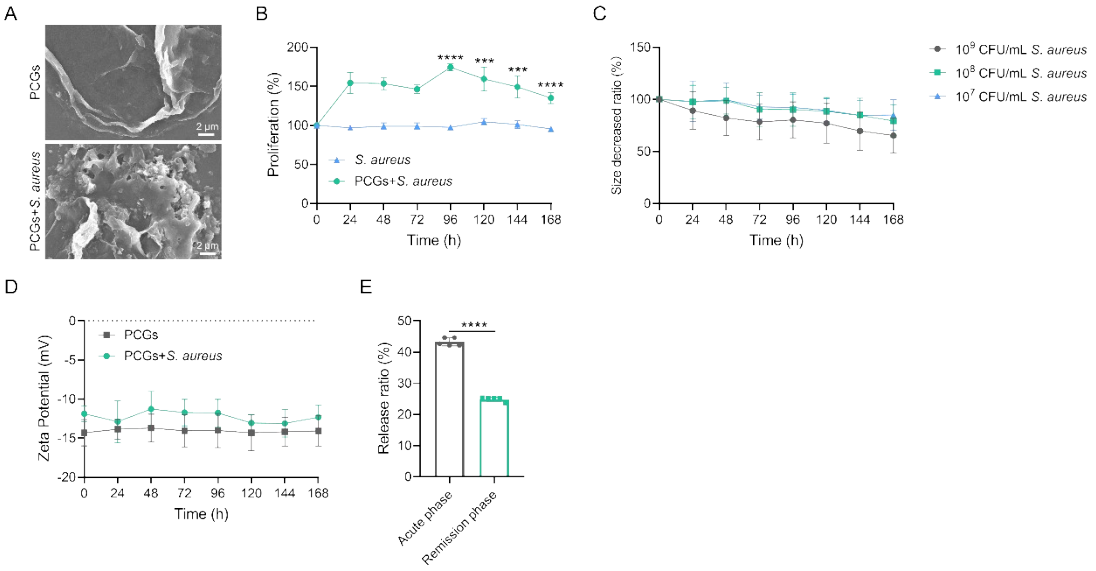

Figure S3. Interaction between PCGs and *S. aureus*. A. Representative SEM images of the microstructure of PCGs with or without *S. aureus* cocultured for 168 h. Scale bar=2 μm. **B.** Proliferation of *S. aureus* during bacterial interaction. **C.** Size decreased ratio of PCGs after incubated with different concentrations of *S. aureus*. **D.** Changes in zeta potential of PCGs during bacterial interaction. **E.** Release ratio of Cy5.5 at acute and remission phase of *S. aureus*-infection *in vivo*. The data are presented as means ± SD. Statistical significance was determined by two-tailed Student's t-tests. ****$p < 0.0001$; ***$p < 0.001$.

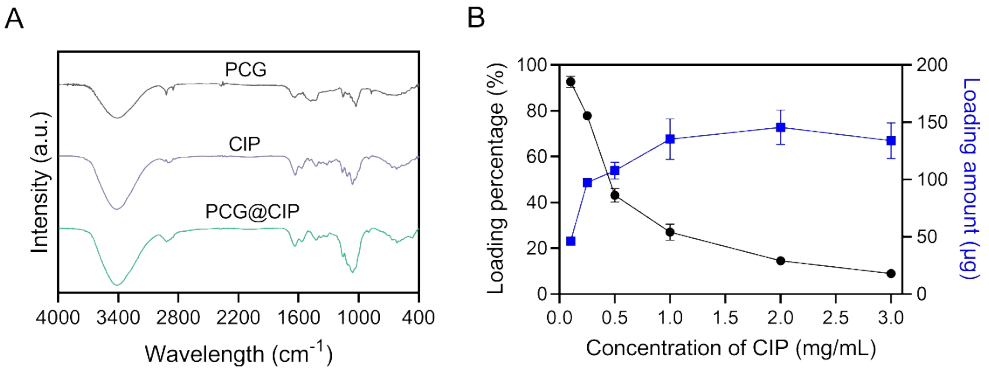

Figure S4. Loading capacity of PCGs to ciprofloxacin. A. Infrared spectrogram of PCG, CIP and PCG@CIP. **B.** The loading amount and loading percentage of CIP into PCGs (n=5). The data are presented as means ± SD.

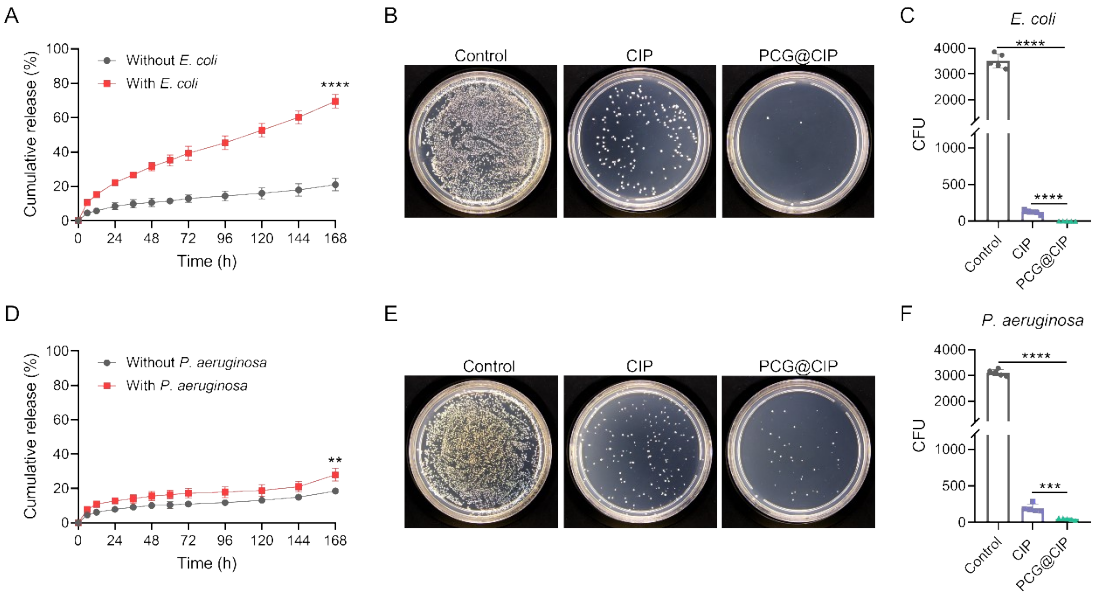

Figure S5. Versatility of PCGs drug delivery system. A. *In vitro* cumulative release profiles of Cy5.5 from Cy5.5-labelled PCGs with or without *E. coli*. **B, C.** Representative photographs of *E. coli* colonies formed on LB-agar plates **(B)** and relevant statistical analysis **(C)** after cocultured with PBS, CIP and PCG@CIP *in vitro* (n=5). **D.** *In vitro* cumulative release profiles of Cy5.5 from Cy5.5-labelled PCGs with or without *P. aeruginosa*. **E, F.** Representative photographs of *P. aeruginosa* colonies formed on LB-agar plates **(E)** and relevant statistical analysis **(F)** after cocultured with PBS, CIP and PCG@CIP *in vitro* (n=5). The data are presented as means ± SD. Statistical significance was determined by two-tailed Student's t-tests and one-way ANOVA with the Tukey post hoc test. ****$p < 0.0001$; ***$p < 0.001$; **$p < 0.01$.

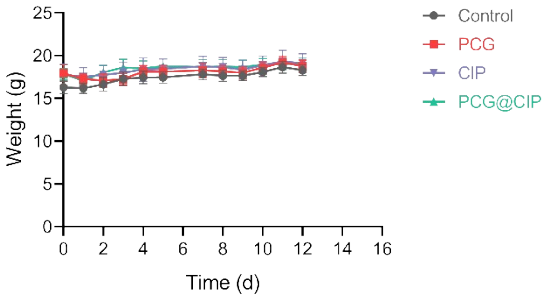

Figure S6. Body weights of mice after different treatments. The data are presented as means ± SD.

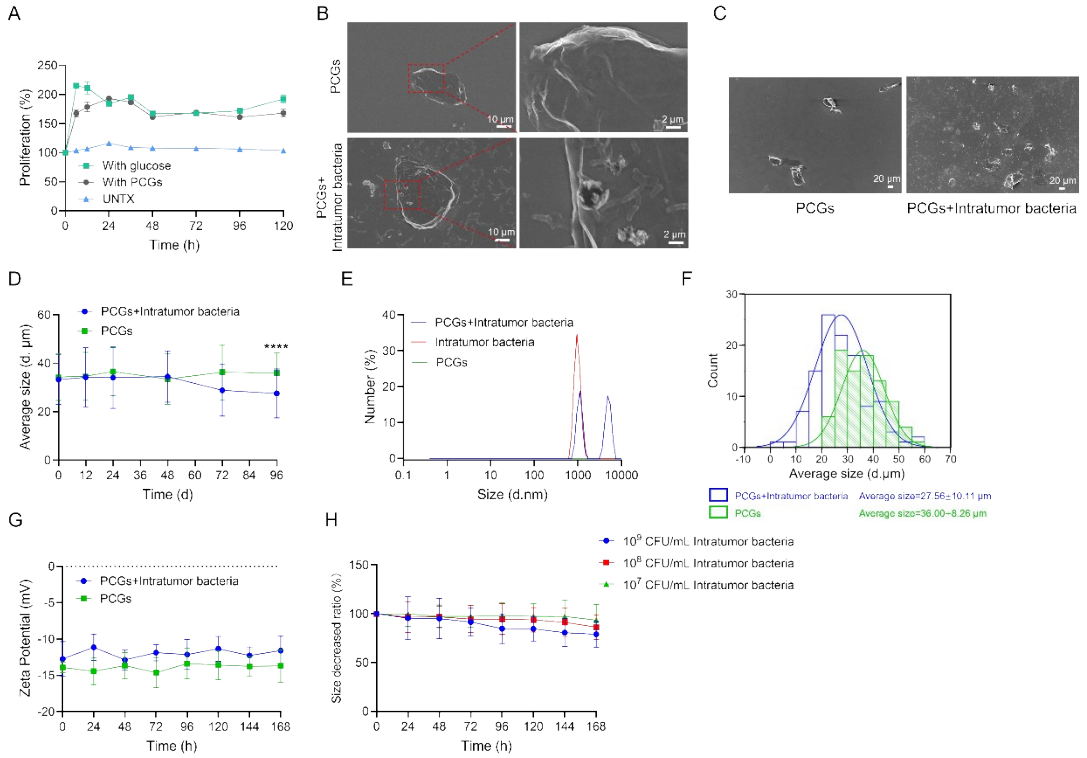

Figure S7. Coactions between PCGs and intratumor bacteria. A. Proliferation of intratumor bacteria. **B.** Representative SEM images of the microstructure of PCGs after cocultured with or without the presence of intratumor bacteria for 96 h. Scale bar=10 μm (left), 2 μm (right). **C.** Representative SEM images of the macrostructure of PCGs after cocultured with intratumor bacteria for 96 h. Scale bar=20 μm. **D.** Average size of PCGs after incubation with intratumor bacteria for different time. **E.** The size of PCGs, intratumor bacteria and PCGs with intratumor bacteria. **F.** The size distribution of PCGs with or without the presence of intratumor bacteria for 96 h according to SEM images. **G.** Changes in zeta potential of PCGs during bacterial interaction. **H.** Size decreased ratio of PCGs after incubated with different concentrations of intratumor bacteria. The data are presented as means ± SD. Statistical significance was determined by two-tailed Student's t-tests. ****$p < 0.0001$.

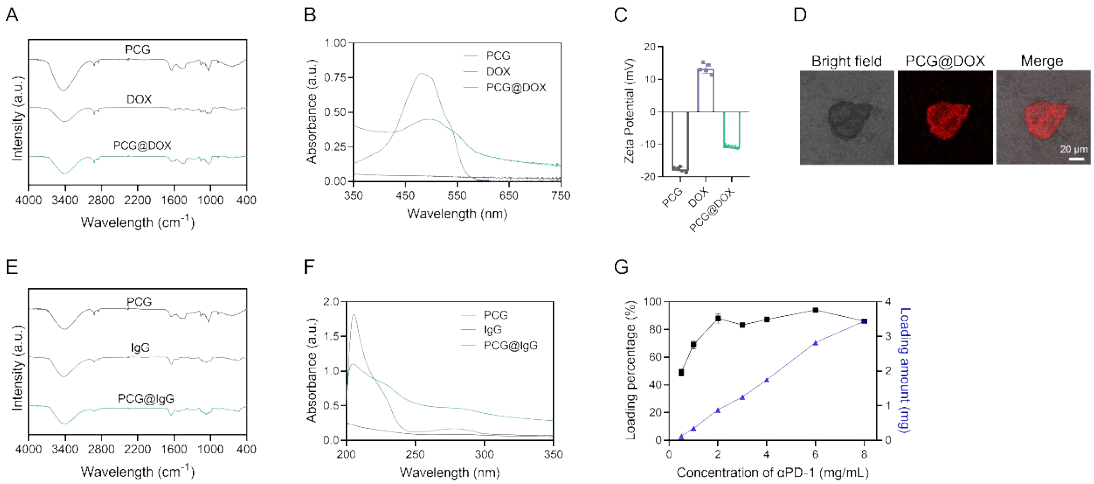

Figure S8. Drug loading properties of PCGs. A. Infrared spectrogram of PCG, DOX and PCG@DOX. **B.** UV-vis absorption of PCG, DOX and PCG@DOX. **C.** The zeta potential of PCG, DOX and PCG@DOX (n=5). **D.** Representative confocal images of PCGs loaded with DOX. Scale bar=20 μm. **E.** Infrared spectrogram of PCG, IgG antibody and PCG@IgG. **F.** UV–vis absorption of PCG, IgG antibody and PCG@IgG. **G.** The loading amount and loading percentage of αPD-1 antibody into PCGs (n=4). The data are presented as means ± SD.

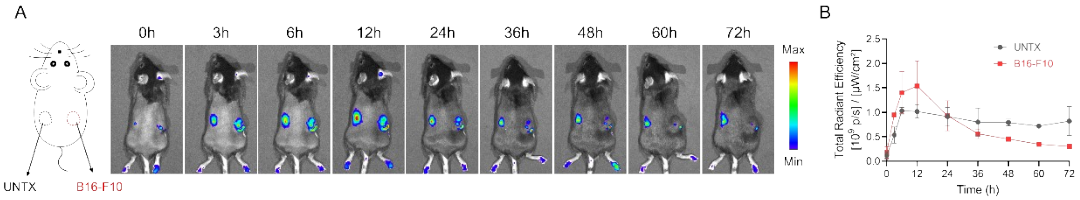

Figure S9. Intratumor bacteria mediated the release of drug *in vivo*. A. Representative fluorescence imaging of tumor-bearing mice after intratumor injection of PCG@IgG-Cy5.5 at different time points. **B.** Quantification of the fluorescence intensity of Cy5.5 at different time points (n=6). The data are presented as means ± SD.

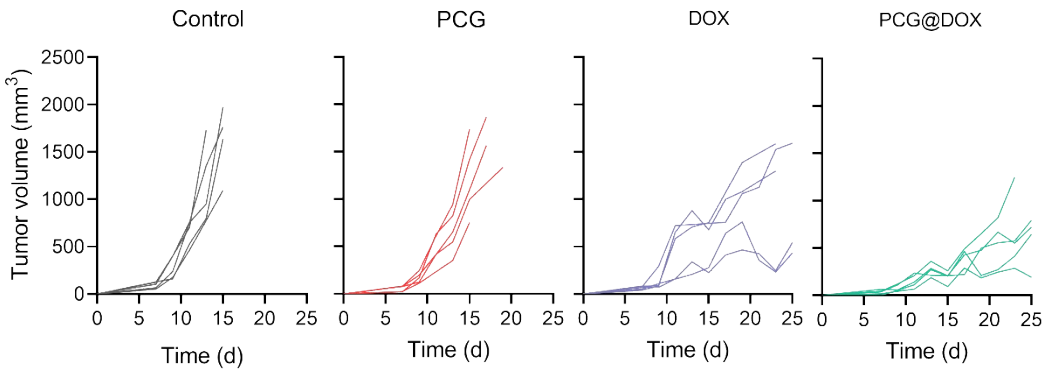

Figure S10. Tumor therapeutic efficacy with PCG@DOX. Individual tumor growth curves after different treatments (n=5).

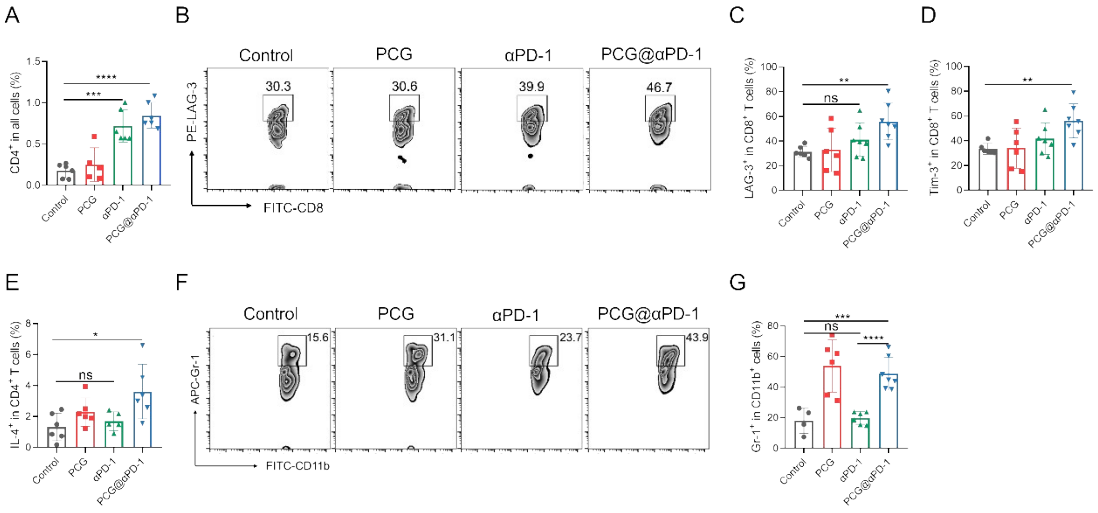

Figure S11. PCG@αPD-1 enhanced the anti-tumor immune responses. A. Corresponding quantitative analysis of $CD4^+$ T cells in the tumor. **B.** Representative flow cytometry plots of LAG-3^+ in $CD8^+$ T cells. **C.** Corresponding quantitative analysis of LAG-3^+ in $CD8^+$ T cells. **D.** Corresponding quantitative analysis of TIM-3^+ in $CD8^+$ T cells. **E.** Corresponding quantitative analysis of IL-4^+ in $CD4^+$ T cells. **F.** Representative flow cytometry plots of Gr-1^+ in $CD11b^+$ cells for tumor. **G.** Corresponding quantitative analysis of Gr-1^+ in $CD11b^+$ cells. The data are presented as means ± SD. Statistical significance was determined by two-tailed Student's t-tests and one-way ANOVA with the Tukey post hoc test. ****$p < 0.0001$; ***$p < 0.001$; **$p < 0.01$; *$p < 0.05$; ns, no significance.

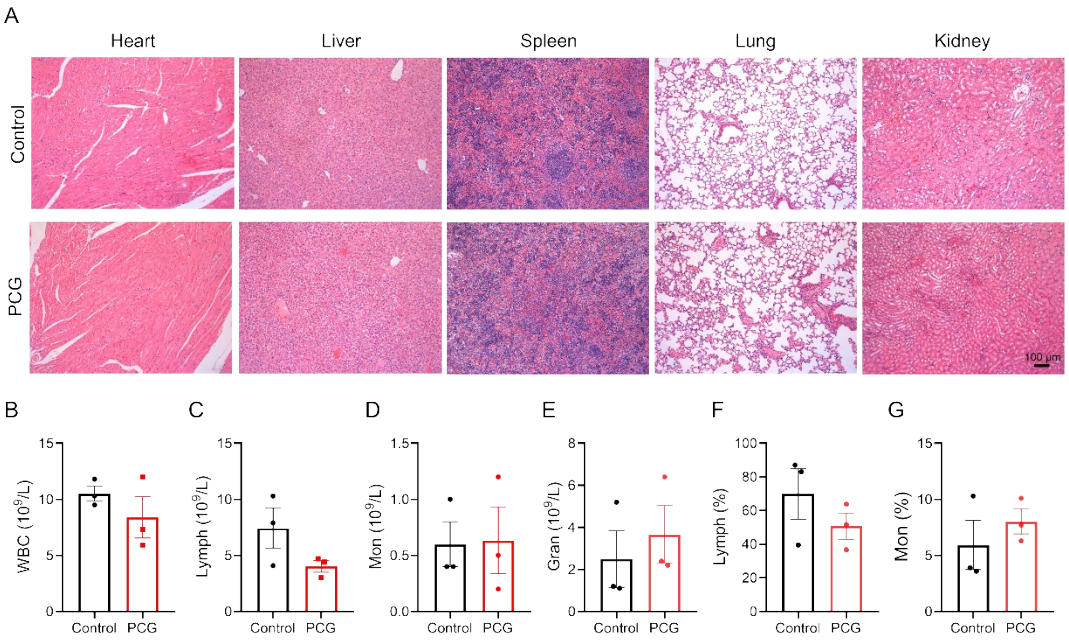

Figure S12. PCGs within good biosecurity. A. HE sections of major organs confirmed the good biosafety of PCGs. Scale bar=100 μm. **B.** Blood routine index after treating with PCGs showed slight changes indicating the good biocompatibility. The data are presented as means ± SD.

Table S1 Materials and antibodies

Material	Manufacturer	Catalog Number
Sodium carbonate anhydrous	Macklin	C10112442
Potassium bromide	ACMEC	P387386CE
α-Cellulose	Aladdin	D2122119
BeyoPure LB Broth (premixed powder)	Beyotime	ST156
Agar	Macklin	C14089442
High Glucose DMEM	Vivacell	2409079
Penicillin-Streptomycin Solution	Seven biotech	SC118-01
Trypsin 0.25% Solution	Seven biotech	SC107-01
PBS	Seven biotech	24EB1002
Ciprofloxacin	TCL	HRKFM-GD
Doxorubicin hydrochloride	Meryer	M12008
Mouse IgG powder	Solarbio	SP031
Cy5.5 NHS ester	Yuanye Bio	S27624
InVivoMAb anti-mouse PD-1(CD279)	BioXcell	BE0146
Western and IP cell lysis buffer	Beyotime	P0013
Rat IgG Total Uncoated ELISA kit	Invitrogen	293062-015
Enhanced BCA Protein Assay Kit	Beyotime	P0009
N01/Pl Live/Dead Bacterial Double Stain Kit	Bestbio	BB-41266
Mouse IFNg Uncoated ELISA kit	Invitrogen	274934-006
Mouse TNF alpha Uncoated ELISA kit	Invitrogen	328775-002
Mouse IL-6 Uncoated ELISA Kit	Invitrogen	330384-001
Crystal Violet Staining Solution	Seven biotech	24BD0480
PE anti-mouse CD45	Biolegend	103105
PE anti-mouse CD3	Biolegend	100206
FITC anti-mouse CD4	Biolegend	100406
APC anti-mouse CD8a	Biolegend	100712
PE anti-mouse CD8a	Biolegend	162304
FITC anti-mouse CD8a	Biolegend	100706
APC anti-human/mouse Granzyme B Recombinant	Biolegend	396408
PE anti-mouse IFN-γ	Biolegend	505808
FITC anti-mouse TNFα	Biolegend	506304
PE/Dazzle$^{TM\ 594}$ anti-mouse CD223 (LAG-3)	Biolegend	125223
APC anti-mouse CD366 (Tim-3)	Biolegend	134008
APC anti-mouse IL-4	Biolegend	504106
APC anti-mouse Ly-6G/Ly-6C (Gr-1)	Biolegend	108412
FITC anti-mouse/human CD11b	Biolegend	101206